

Optimization of SAM Head Phantom for Compact Antenna Test Ranges

Jingtian Xi, Corbett Rowell, Jose M. Fortes, Fereshteh Rouholahnejad, Benoit Derat, and Niels Kuster

Abstract – Over-the-air (OTA) performance evaluations of devices operating at frequencies greater than 6 GHz are typically performed in the compact antenna test ranges (CATRs) with head and hand phantoms. However, existing specific anthropomorphic mannequin (SAM) head phantoms do not meet the quiet zone and weight restrictions of CATRs. In this study, we investigated the feasibility of reducing the size and weight of the SAM head while keeping the effect on all standard OTA performance parameters minimal, i.e., deviations compared to the full-head phantom less than ± 0.2 dB.

1. Introduction

Fifth Generation New Radio (5G NR) networks and devices, complying with the Third Generation Partnership Project (3GPP) standards [1], are currently being released into the market. With the addition of the millimeter wave frequency range 2 (5G NR FR2) band, radiofrequency (RF) conformance and performance must be tested in a radiated, over-the-air (OTA) environment [2]. 3GPP is developing FR2 OTA testing methods, which are currently based on an indirect far-field setup using the compact antenna test ranges (CATRs). It has unique features, such as a compact footprint, and supports all types of RF measurements with low measurement uncertainty while still providing a good dynamic range [3, 4]. The Cellular Telecommunications Industry Association (CTIA) is also working on new millimeter wave OTA testing methods and plans to extend the frequency range of the specific anthropomorphic mannequin (SAM) head phantom and the hand phantoms to above 6 GHz to enable device performance testing in realistic usage scenarios.

However, it is difficult to adopt full-sized head phantoms in CATR systems because of limitations regarding the weight of the load (i.e., phantoms plus the device under test [DUT]) supported by the positioner and the size of the quiet zone provided by the test range.

Manuscript received 31 August 2020.

Jingtian Xi is with the IT²IS Foundation, Zurich, Switzerland; e-mail: xi@itis.swiss.

Corbett Rowell, Jose M. Fortes, and Benoit Derat are with Rohde & Schwarz GmbH & Co. KG, Munich, Germany; e-mail: corbett.rowell@rohde-schwarz.com, jose.fortes@rohde-schwarz.com, benoit.derat@rohde-schwarz.com.

Fereshteh Rouholahnejad is with Schmid & Partner Engineering AG, Zurich, Switzerland; e-mail: rouholahnejad@speag.swiss.

Niels Kuster is with the IT²IS Foundation, Zurich, Switzerland, and with the Swiss Federal Institute of Technology, ETH Zurich, Zurich, Switzerland; e-mail: kuster@itis.swiss.

Although modern CATR systems can support centered load weights of up to 8 kg [5], there are other implementations with limited load capacities of 2–4 kg, making them incapable of handling the full SAM head, which has a weight of around 6 kg. Considering that modern CATR systems provide quiet zones of up to 30 cm in diameter, the size of the full SAM head requires the DUT to be positioned offset far from the center of the coordinate system, where it may even lie outside the quiet zone, leading to increased measurement uncertainty. Bringing the DUT closer to the center may also not be an option, as this could introduce torque that does not comply with the positioner specifications.

2. Development Methodology

In this study, we used the finite-difference time-domain solver in Sim4Life V5.0 (ZMT Zurich MedTech AG) to investigate the feasibility of substantially reducing the size and weight of the full silicone-carbon-based SAM head to allow positioning the DUT in the center of the quiet zone for millimeter wave OTA tests while minimizing the impact on OTA performance evaluation. The OTA performance of antennas in a virtual cellphone placed in the tilted talk position (6° from the touch position) against the full-head phantom was compared to that for partial-head phantoms in which materials on the shadow side were progressively removed (see Figure 1) until significant differences in OTA performance were observed. In a second step, the influence of removing the material inside the head phantom on the OTA performance parameters was investigated. The weights (excluding the stand) of the half-head phantom, the 3/8-head phantom, and the 3-cm-thick hollow half-head phantom are 3.1 kg, 2.0 kg, and 2.1 kg, respectively. The electrical properties of the phantom material used in this study are provided in Table 1.

Differences in performance between the full-head phantom and the partial-head phantoms were derived for all standard OTA performance parameters [6]: total radiated power, mismatch efficiency, radiation efficiency, maximum gain, total isotropic sensitivity, near-horizon partial radiated power (radiated over $\pm 30^\circ$ and $\pm 45^\circ$ near the horizon, hereinafter NHPRP30deg and NHPRP45deg, respectively), upper hemisphere radiated power, and partial Global Navigation Satellite System radiated power. To better analyze the effect of the head phantom modification, we added a parameter that characterizes the power radiated toward the shadow side (i.e., toward the +Y direction), as shown in Figure 2. The new parameter was extracted from 45° to 135° for both the elevation angle θ and the azimuth angle ϕ .

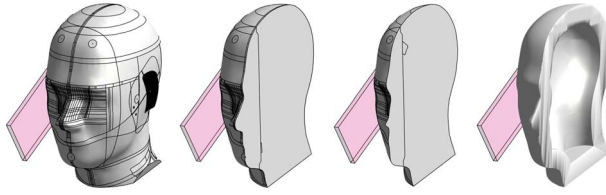


Figure 1. From left to right: full-head, half-head, 3/8-head, hollow half-head phantom (3 cm thick). The position of the virtual cellphone is indicated by the pink box.

Table 1. Electrical properties of the phantom material.

Frequency (GHz)	Relative permittivity	Conductivity (S/m)
6	20.6	2.63
10	18.9	3.44
38.5	15.3	7.53
90	13.9	10.8

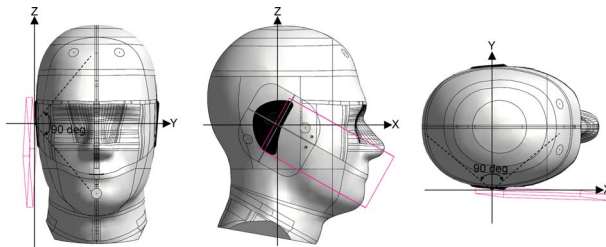


Figure 2. From left to right: front view, right side view, top view of NOPRP45deg defined in the context of the CTIA coordinate system. The position of the virtual cellphone is indicated by the pink wireframe.

Table 2. Dimensions of 6 GHz, 10 GHz, and 90 GHz dipoles. Gap width corresponds to the small feeding gap between two dipole arms.

Frequency (GHz)	Arm length (mm)	Arm radius (mm)	Gap width (mm)
6	11.3	0.278	0.05
10	6.79	0.167	0.03
90	0.754	0.0185	0.003

In analogy to NHPRP45deg, we call the new parameter NOPRP45deg, where NOPRP stands for “Near Opposite Partial Radiated Power.” Deviations in the standard OTA performance parameters and NOPRP45deg (all normalized to the same conducted power) due to the reduction of the phantom size and weight indicate whether the partial-head phantoms qualify as acceptable representations of the full-head phantom.

Four antennas were selected to cover the frequency range from 6 GHz to 100 GHz: 6 GHz dipole, 10 GHz dipole, 90 GHz dipole, and 38.5 GHz patch array. The dimensions of the three dipole antennas are listed in Table 2. For the middle frequency, we simulated the 38.5 GHz validation patch array. It is a series-fed eight-element design implemented on a RO4350B substrate with a size of $46.5 \text{ mm} \times 14 \text{ mm} \times 0.254 \text{ mm}$. The array

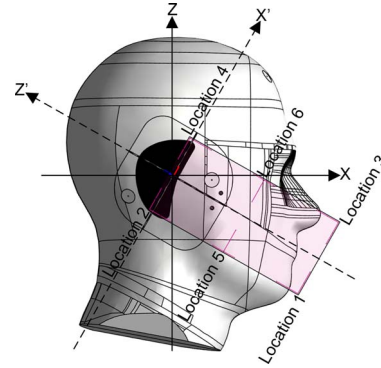


Figure 3. The locations and orientations investigated with the dipoles represented by pink rods and the virtual cellphone indicated by the transparent pink box. The CTIA coordinate system (illustrated by X and Z axes) and the modeling coordinate system (illustrated by X' and Z' axes) are also shown.

lies along the short edge of a ground plane with a size of approximately $57.7 \text{ mm} \times 73 \text{ mm}$ and provides a directivity of 15.5 dBi in free space.

The influence of the antenna positioning was addressed by placing the antennas at multiple locations and orientations in a virtual cellphone with dimensions of $158 \text{ mm} \times 77 \text{ mm} \times 8 \text{ mm}$ (obtained from our survey of popular commercial smart phones). All three dipoles (6 GHz, 10 GHz, and 90 GHz dipoles) were positioned at six locations within the virtual cellphone: at four corners and at the centers of two long edges (see Figure 3). Moreover, two orientations (X' and Z') were studied for the dipoles. The 38.5 GHz patch array was positioned at four corners of the virtual cellphone with the orientations that allow exposing the coaxial connector for any potential measurement (see Figure 4).

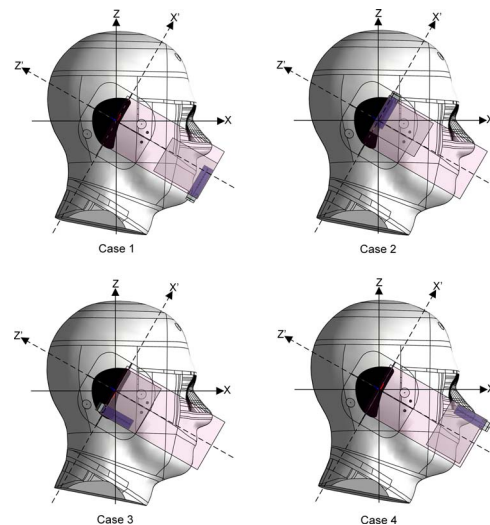


Figure 4. The four cases investigated with the 38.5 GHz patch array and the virtual cellphone indicated by the transparent pink box. The CTIA coordinate system (illustrated by X and Z axes) and the modeling coordinate system (illustrated by X' and Z' axes) are also shown.

Table 3. Maximum absolute deviations (in dB) between the results of all parameters in [6] and NOPRP45deg obtained with the half-head phantom and the full-head phantom for the three dipoles and the 38.5 GHz patch array, with all study cases taken into account.

Antenna	Parameters in [6]	NOPRP45deg
6 GHz dipole	0.09	0.14
10 GHz dipole	0.16	0.15
90 GHz dipole	0.00	0.11
38.5 GHz patch array	0.20	0.14

3. Results

In a first step, the absolute deviations between the results obtained with the full-head phantom and the half-head phantom were derived for all study cases. The 12 cases for the dipoles are shown in Figure 3, and the four cases for the patch array are shown in Figure 4. The maximum absolute deviations found out of all study cases for the three dipoles and the 38.5 GHz patch array are provided in Table 3. The maximum absolute deviations for all standard OTA performance parameters are mostly observed on the maximum gain. The results show that the deviations of the half-head phantom with respect to the full-head phantom are within 0.2 dB for all OTA performance parameters specified in [6] as well as NOPRP45deg. This will only minimally impact the overall head-phantom uncertainty of 0.7 dB to 1 dB [7].

The feasibility of further reducing the phantom size to a 3/8 head was studied with the 10 GHz dipole in four cases (X'1, X'3, Z'1, and Z'3), which are the cases that are the most sensitive to the phantom size reduction. The absolute deviations between results of the 3/8-head phantom and the full-head phantom are provided in Table 4. They reveal that, when the phantom size decreases from a half head to a 3/8 head, deviations for NOPRP45deg become noticeably larger. This can be attributed to a smaller cross section and stronger diffraction. Moreover, deviations for OTA performance parameters specified in [6] are up to 0.31 dB. Therefore, the half head can be regarded as the minimum acceptable phantom size for reliable OTA testing at frequencies above 6 GHz.

In a second step, the material inside the half-head phantom was removed, because the weight of the half-head phantom (≈ 3.5 kg, including the stand) is still too heavy for some CATR systems. The resulting head is a

Table 4. Absolute deviations (in dB) between the results of all parameters in [6] and NOPRP45deg obtained with the 3/8-head phantom and the full-head phantom in four cases for the 10 GHz dipole. The case number indicates the orientation and the location (see Figure 3) of the dipole.

Case no.	Parameters in [6]	NOPRP45deg
X'1	0.16	0.50
X'3	0.25	0.87
Z'1	0.24	0.73
Z'3	0.31	0.88

Table 5. Maximum absolute deviations (in dB) between the results of all parameters in [6] and NOPRP45deg obtained with the 3-cm-thick hollow half-head phantom and the full-head phantom for the three dipoles and the 38.5 GHz patch array, with all study cases taken into account.

Antenna	Parameters in [6]	NOPRP45deg
6 GHz dipole	0.10	0.96
10 GHz dipole	0.15	0.26
90 GHz dipole	0.06	0.12
38.5 GHz patch array	0.20	0.14

conformal material layer with a thickness of 3 cm (see the last plot in Figure 1). The maximum absolute deviations between results obtained with the 3-cm-thick hollow half-head phantom and the full-head phantom found in all study cases for the three dipoles and the 38.5 GHz patch array are provided in Table 5. They demonstrate that the deviations of the 3-cm-thick hollow half-head phantom with respect to the full-head phantom lie within 0.2 dB for all OTA performance parameters specified in [6]. Deviations for NOPRP45deg observed on the 6 GHz dipole and the 10 GHz dipole are noticeably larger than those found on the (solid) half-head phantom; however, large deviations are observed only in the cases X'4 and Z'4, as shown in Table 6. The dipole location in the two cases results in a strong radiation shadow. As shown in Figures 5 and 6, NOPRP45deg in the two cases corresponds to the nulls of the radiation patterns, and hence the value of NOPRP45deg becomes very small. Further reducing the thickness of the hollow half-head would lead to larger deviations for NOPRP45deg. Taking the 10 GHz dipole, for instance, with a material layer thickness of 2 cm, the maximum absolute deviation for NOPRP45deg with respect to the full head is 3.26 dB.

4. Conclusions

This study demonstrates that a hollow half-head phantom with a conformal thickness of at least 3 cm

Table 6. Absolute deviations (in dB) between the results of NOPRP45deg obtained with the 3-cm-thick hollow half-head phantom and the full-head phantom for the 6 GHz dipole and the 10 GHz dipole. The case number indicates the orientation and the location (see Figure 3) of the dipoles.

Case no.	6 GHz dipole	10 GHz dipole
X'1	0.06	0.07
X'2	0.01	0.14
X'3	0.09	0.06
X'4	0.84	0.26
X'5	0.00	0.01
X'6	0.02	0.00
Z'1	0.15	0.14
Z'2	0.14	0.06
Z'3	0.11	0.13
Z'4	0.96	0.22
Z'5	0.03	0.10
Z'6	0.03	0.09

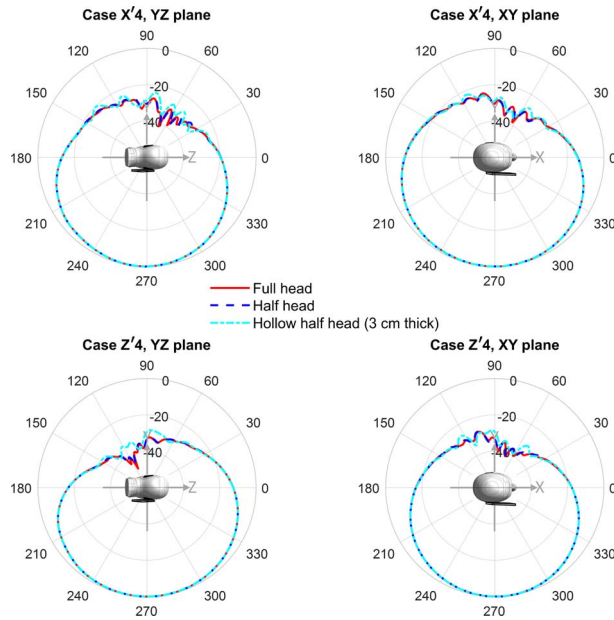


Figure 5. Normalized total-gain patterns (in dB) of the 6 GHz dipole for the cases X'4 and Z'4. The CTIA coordinate system, the head phantom, and the virtual cellphone are also shown.

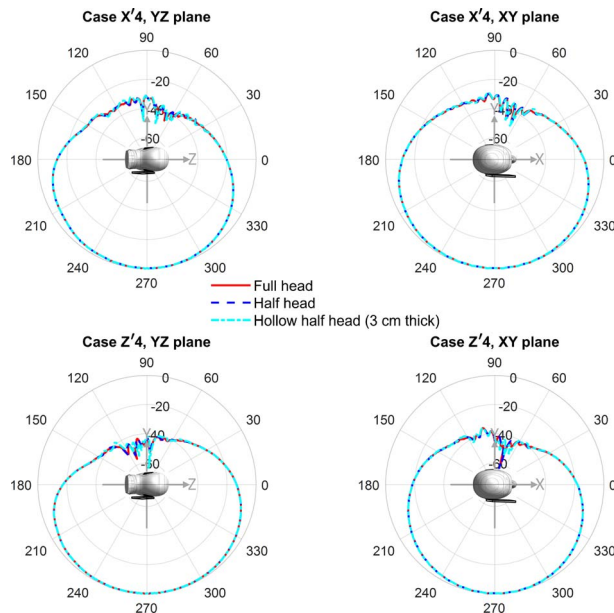


Figure 6. Normalized total-gain patterns (in dB) of the 10 GHz dipole for the cases X'4 and Z'4. The CTIA coordinate system, the head phantom, and the virtual cellphone are also shown.

well represents the full-head phantom for the OTA performance parameters as defined by the standardization groups at frequencies greater than 6 GHz. This indicates that the full SAM head can be optimized in size and weight for millimeter wave OTA tests. Compared with the full-head phantom, the 3-cm-thick hollow half-head phantom enables us to reduce the phantom size by 50% and the phantom weight by more than 60% to ≈ 2.5 kg (including the stand) [8], with deviations in the standard OTA performance parameters $< \pm 0.2$ dB. The numerical results will be experimentally verified using the Rohde and Schwarz ATS1800C CATR with the full-head phantom and the optimized hollow half-head phantom.

5. References

- 3GPP, "Release 16," <https://www.3gpp.org/release-16> (Accessed 28 August 2020).
- A. V. Lopez, A. Chervyakov, G. Chance, S. Verma, and Y. Tang, "Opportunities and Challenges of mmWave NR," *IEEE Wireless Communications*, **26**, 2, April 2019, pp. 4-6, doi: 10.1109/MWC.2019.8700132.
- S. F. Gregson and C. G. Parini, "Use of OTA System Performance Metrics in the Design & Optimization of CATRs for 5G Testing," 2019 Antenna Measurement Techniques Association Symposium (AMTA), San Diego, CA, USA, 6-11 October 2019, pp. 1-6, doi: 10.23919/AMTAP.2019.8906455.
- S. F. Gregson and C. G. Parini, "Compact Antenna Test Ranges: The Use of Simulation and Post-Processing Techniques in Support of 5G OTA Testing," 2019 13th European Conference on Antennas and Propagation (EuCAP), Kraków, Poland, 31 March to 5 April 2019, pp. 1-1.
- Rohde & Schwarz, "Over-the-Air Antenna Test Solutions," https://www.rohde-schwarz.com/lt/products/test-and-measurement/over-the-air-antenna-test-solutions/over_the_air_antenna_testers_103249.html (Accessed 28 August 2020).
- CTIA, *Test Plan for Wireless Device Over-the-Air Performance—Method of Measurement for Radiated RF Power and Receiver Performance*, version 3.8.2, CTIA Certification Program, Washington, DC, April 2019.
- E. Ofli, N. Chavannes, and N. Kuster, "The Uncertainties and Repeatability Limitations of Transmitter and Receiver Performance Assessments Posed by Head Phantoms," IEEE International Workshop on Antenna Technology Small Antennas and Novel Metamaterials, White Plains, NY, USA, 6-8 March 2006, pp. 349-352, doi: 10.1109/IWAT.2006.1609047.
- SPEAG, "mmWave $\frac{1}{2}$ SAM Phantoms Extend OTA Testing in CATR for 5G FR2 Devices," <https://speag.swiss/news-events/news/measurement/mmwave-sam-phantoms-extend-ota-testing-in-catr-for-5g-fr2-devices/> (Accessed 28 August 2020).